ELECTRONIC SUPPORTING INFORMATION

FRET-Based Metal Ion Sensing by Crown-Containing Bisstyryl Dye

Maria A. Ustimova, Anna Yu. Lebedeva, Yuri V Fedorov, Daria V. Berdnikova, Olga A. Fedorova

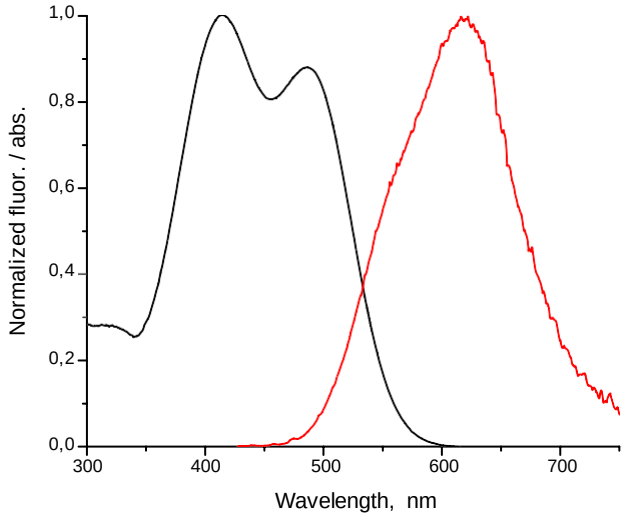

Figure S1. Normalized absorption and fluorescence spectra of **1**, λ_{ex}= 415 nm, c = 5 μM, MeCN, 20 °C.

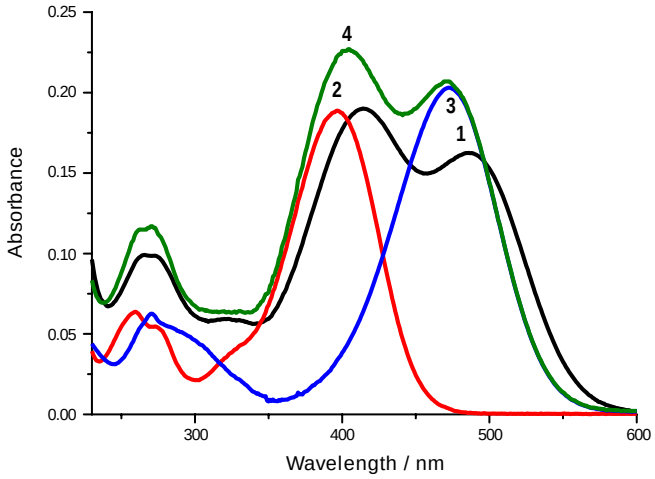

Figure S2. Absorption spectra of bischromophoric dye **1** (1); monochromophoric dye **2** (2); monochromophoric dye **3** (3); theoretical sum of monochromophoric dyes **2** and **3** (4), $C_{\mathbf{1\text{-}3}}$ = 5 μM, MeCN, 20 °C.

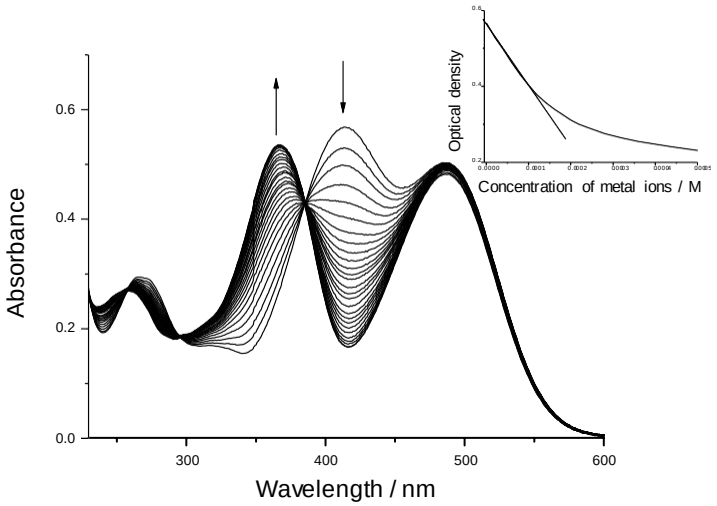

Figure S3. Spectrophotometric titration of **1** with $Mg(ClO_4)_2$ ($c_{\mathbf{1}}$ = 20 μM, $c_{Mg2+}/c_{\mathbf{1}}$ = 0–182) in MeCN at 20 °C, the insert shows linear range of optical density at 415 nm versus concentration of Mg^{2+}.

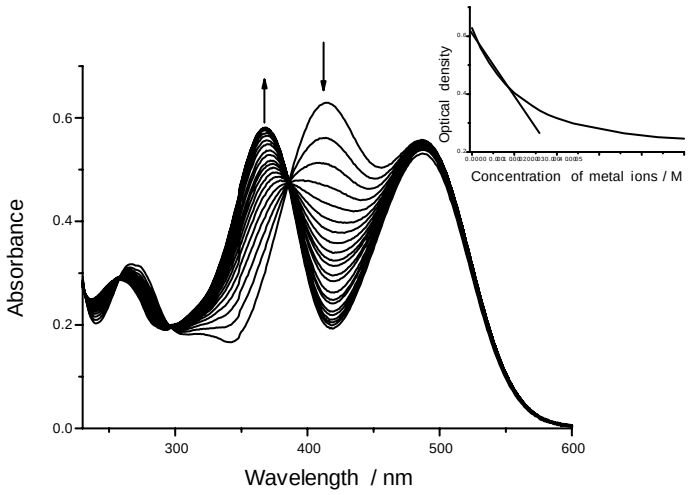

Figure S4. Spectrophotometric titration of **1** with $NaClO_4$ ($c_{\mathbf{1}}$ = 20 μM, $c_{Na+}/c_{\mathbf{1}}$ = 0–265) in MeCN at 20 °C, the insert shows linear range of optical density at 415 nm versus concentration of Na^{+}.

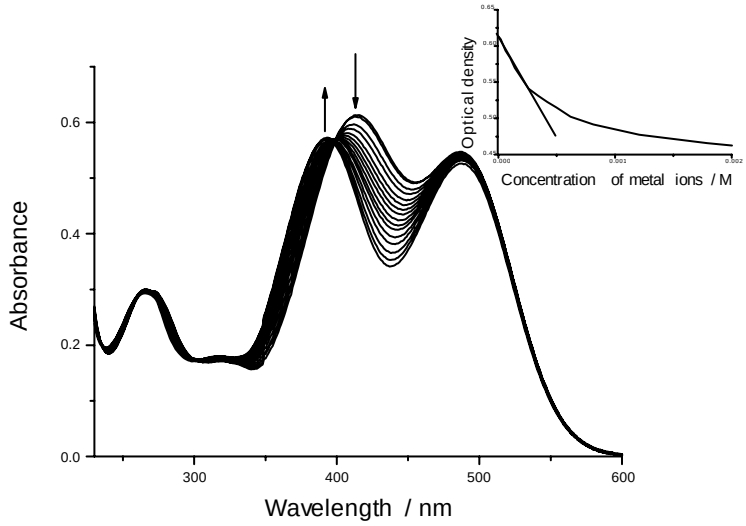

Figure S5. Spectrophotometric titration of **1** with $LiClO_4$ ($c_{\mathbf{1}}$ = 20 μM, $c_{Li+}/c_{\mathbf{1}}$ = 0–131) in MeCN at 20 °C, the insert shows linear range of optical density at 415 nm versus concentration of Li^+.

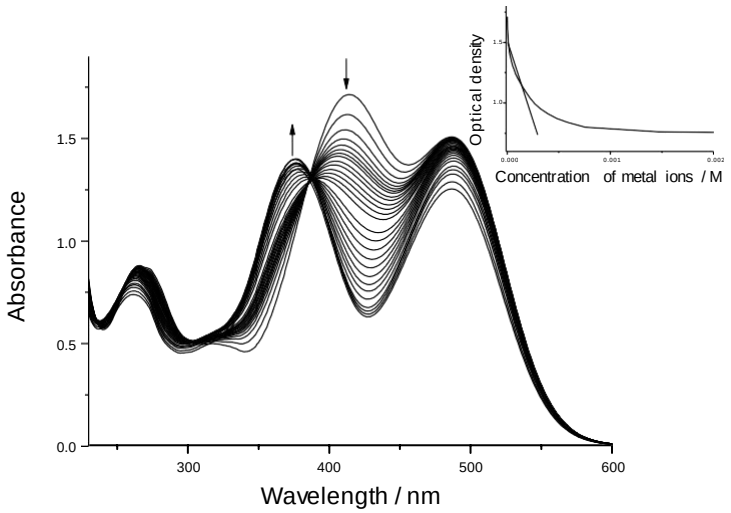

Figure S6. Spectrophotometric titration of **1** with $Ba(ClO_4)_2$ ($c_{\mathbf{1}}$ = 50 μM, $c_{Ba2+}/c_{\mathbf{1}}$ = 0–193) in MeCN at 20 °C, the insert shows linear range of optical density at 415 nm versus concentration of Ba^{2+}.

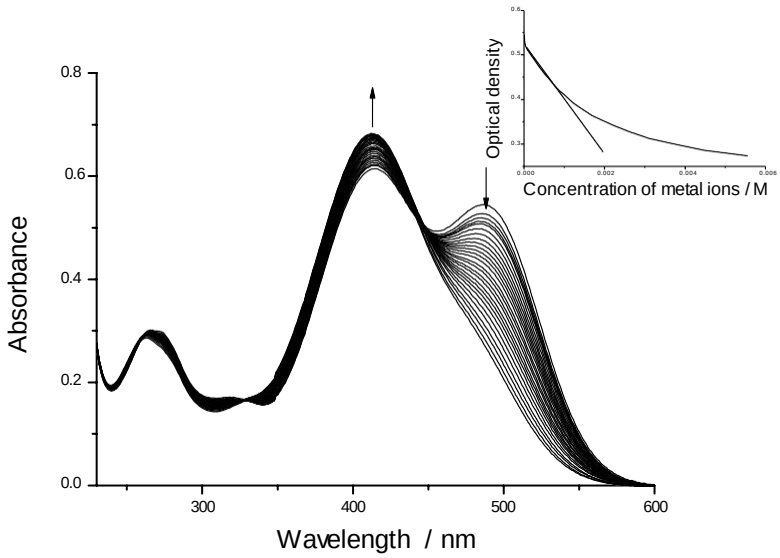

Figure S7. Spectrophotometric titration of **1** with $AgClO_4$ ($c_{\mathbf{1}}$ = 20 μM, $c_{Ag+}/c_{\mathbf{1}}$ = 0–294) in MeCN at 20 °C, the insert shows linear range of optical density at 415 nm versus concentration of Ag^+.

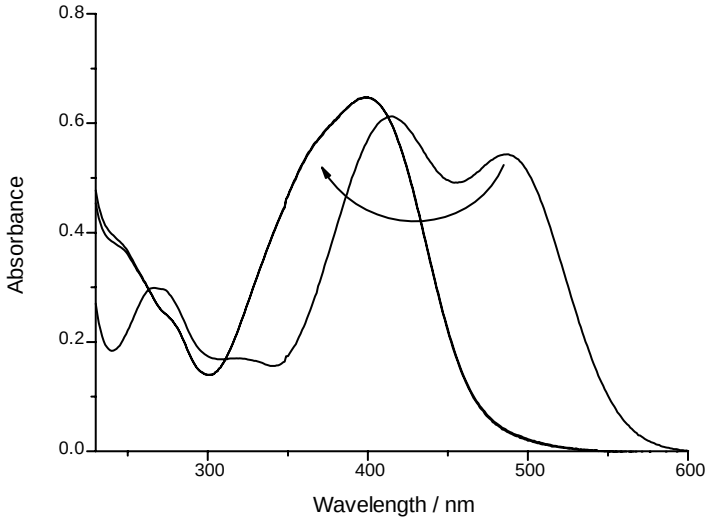

Figure S8. Spectrophotometric titration of **1** with $Hg(ClO_4)_2$ ($c_{\mathbf{1}}$ = 20 μM, $c_{Hg}{}^{2+}/c_{\mathbf{1}}$ = 0–2) in MeCN at 20 °C.

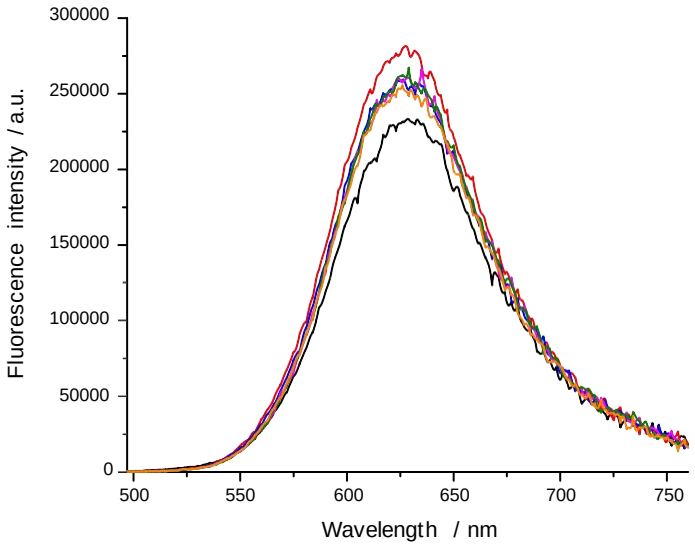

Figure S9. Fluorescence spectra of bischromophoric dye **1** (black); complex **1**·Mg^{2+} (red); complex **1**·Ca^{2+} (blue); complex **1**·Na^{+} (pink); complex **1**·Li^{+} (green); complex **1**·Ba^{2+} (orange). In all cases ligand concentration c = 5 μM, cation concentration c = 5 mM, excitation at 487 nm, acetonitrile, 20 °C.

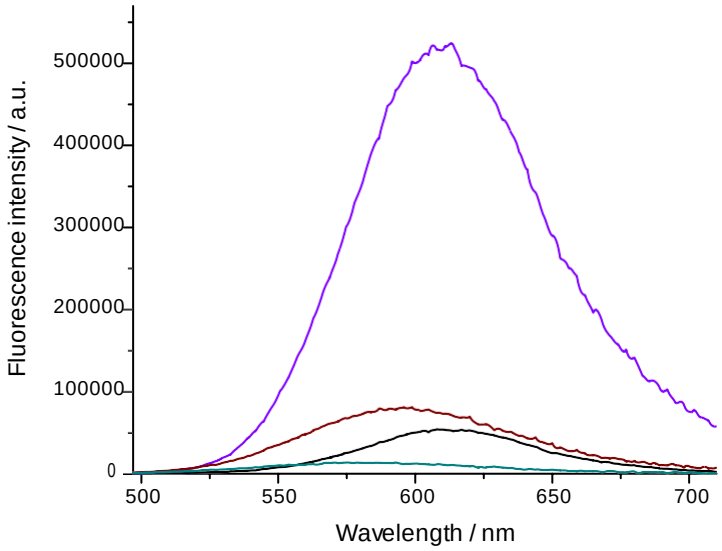

Figure S10. Fluorescence spectra of bis-chromophoric dye **1** (black); complex **1**·Hg^{2+} (brown); complex **1**·Ag^{+} (violet); complex **1**·H^{+} (cyan). In all cases ligand concentration c = 5 μM, cation concentration c = 5 mM (except for Hg^{2+} c = 0.02 mM), excitation at 487 nm, acetonitrile, 20 °C.

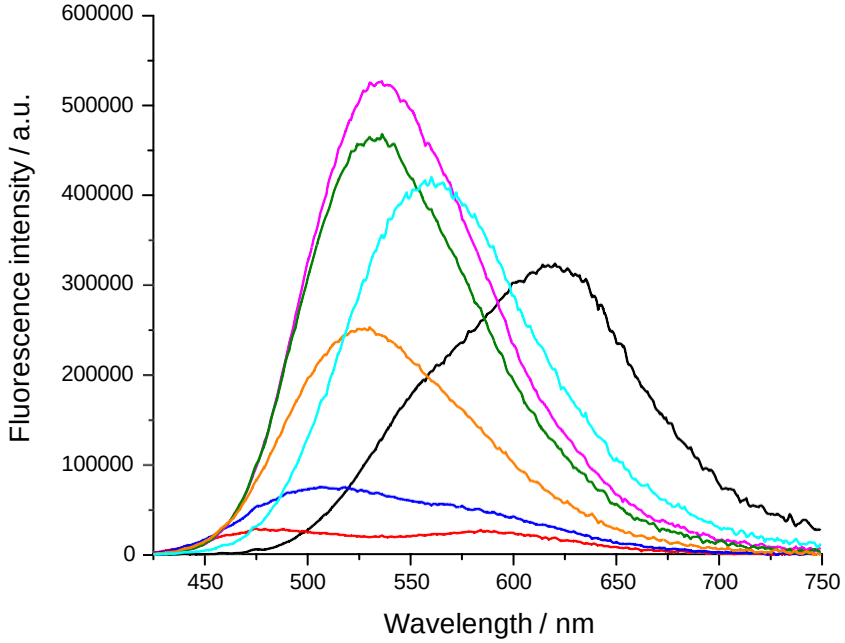

Figure S11. Fluorescence spectra of bis-chromophoric dye **1** (black); complex **1**·H^+ (cyan); complex **1**·H^+·Mg^{2+} (red); complex **1**·H^+·Ca^{2+} (blue); complex **1**·H^+·Na^+ (pink); complex **1**·H^+·Li^+ (green); complex **1**·H^+·Ba^{2+} (orange). In all cases the ligand concentration c = 5 μM, the cation concentration c = 5 mM (except for H^+ c =0.5 mM), excitation at 415 nm, acetonitrile, 20 °C.

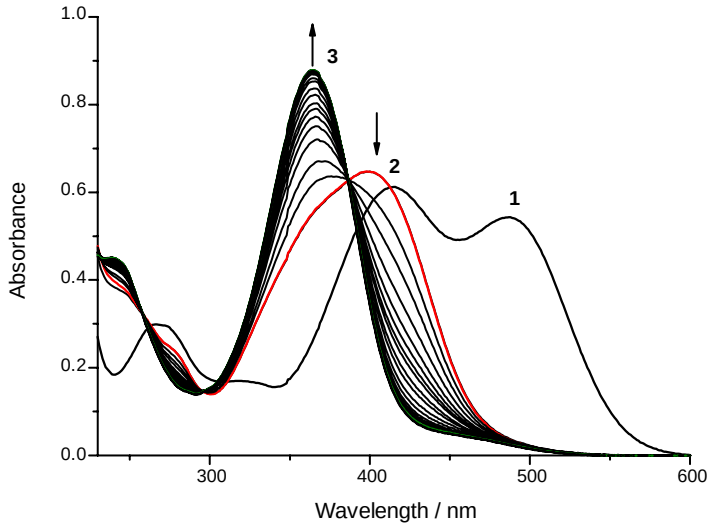

Figure 12. Spectrophotometric titration of complex **1**·Hg^{2+} (2) with $Mg(ClO_4)_2$ ($c_{\mathbf{1}\cdot Hg}^{2+}$ = 20 μM, $c_{Mg}^{2+}/c_{\mathbf{1}\cdot Hg}^{2+}$ = 0–111) in MeCN at 20 °C, curve (1) shows the spectrum of initial dye **1**.

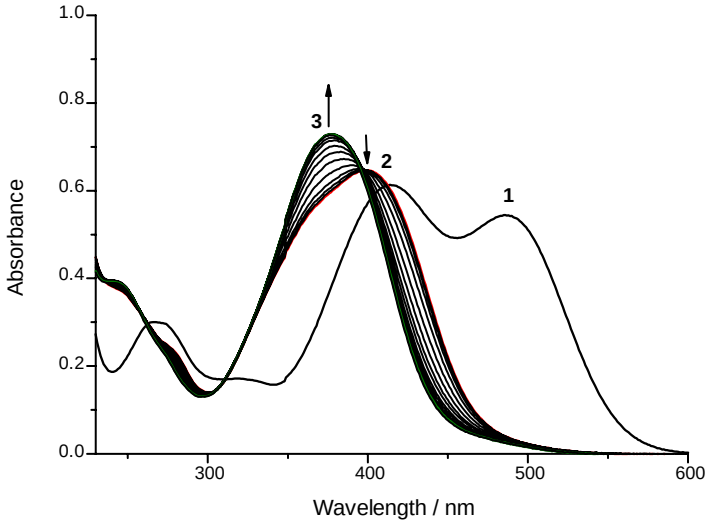

Figure S13. Spectrophotometric titration of complex **1**·Hg^{2+} (2) with $Na(ClO_4)$ ($c_{\mathbf{1}\cdot\mathbf{Hg}}^{2+}$ = 20 μM, $c_{Na}{}^{+}/c_{\mathbf{1}\cdot\mathbf{Hg}}{}^{2+}$ = 0–243) in MeCN at 20 °C, curve (1) shows the spectrum of initial dye **1**.

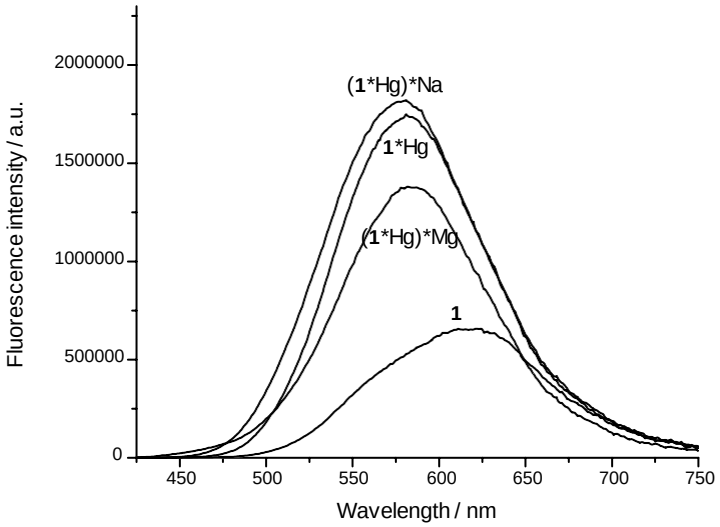

Figure S14. Fluorescence spectra of bis-chromophoric dye **1** (1), complex **1**·Hg^{2+}; complex **1**·Hg^{2+}·Mg^{2+}, complex **1**·Hg^{2+}·Na^{+}; λ_{ex} = 415 nm; $C_{\mathbf{1}}$ = 20 μM, $C_{Hg}{}^{2+}$ = 20 μM, $C_{Mg}{}^{2+}$ = 0.2 mM, , $C_{Na}{}^{+}$ = 0.4 mM. MeCN, 20 °C.